A Single-Pore Model for Gas-Solid Noncatalytic Reactions

P. A. RAMACHANDRAN
and
J. M. SMITH
Department of Chemical Engineering
University of California
Davis, California 95616

Analysis of single-pore behavior in a porous pellet of reactant is used to develop a new model for predicting the conversion-time relationship for gas-solid noncatalytic reactions. The model accounts for the influence of pore diffusion, diffusion through the product layer which builds upon the pore walls, and surface reaction. By focusing attention on one pore, it is possible to include the effects of the changes in pore geometry that occur during reaction. Thus, both pore-mouth closure and uniform deposition of product throughout the pellet can be predicted by using appropriate values for the diffusional and physical properties of the reaction system. The key parameters of the model are the effective pore length and effective diffusivity in the product layer. Numerical values of these quantities can be approximated from measurements of the pore volume and surface are of the unreacted and reacted forms of the pellet, or they may be evaluated from a limited amount of conversion vs. time data. The use of the model for predicting conversion-time curves is illustrated with available data for the reduction of nickel oxide pellets with carbon monoxide and for the reaction of sulfur dioxide with calcium carbonate.

SCOPE

Although the sharp interface model has been used extensively to analyze the behavior of noncatalytic gas-solid reactions, it does not account for the structural characteristics of the solid. In recent years, models incorporating these characteristics have been developed; the pore model (Szekely and Evans, 1970; Chu, 1972) and the grain model (Calvelo and Smith, 1971; Szekely and Evans, 1970) illustrate the key developments in this area. These models do not consider the effect of changes in structure during reaction, that is, changes in pore geometry caused by reaction, although such changes are important in many instances. The only published papers accounting for changes in pore geometry appear to be those of Petersen (1957) and Hashimoto and Silveston (1973, 1973*a*) who analyzed a gasification type of reaction. The reaction scheme studied was such that all the products were gaseous and hence the work has limited applicability to a general noncatalytic gas-solid reaction.

Chemical reaction may result in a more open pore structure when the molal volume of the product formed is less than that of the reactant. Such a reaction scheme applies to reduction of some oxides and gasification types of processes. Alternately, the effect of chemical reaction may be to form a more dense pore structure resulting in a decrease in porosity. Examples are the hydrofluorination of uranium dioxide and sulfation of calcium oxide. The rate of reaction and the conversion-time relations are significantly affected by such changes. In an extreme case pore closure can occur, resulting in incomplete conversion of the solid reactant. In the present paper a single-pore model is developed to account for structural changes due to reaction. The key feature of this work is that by focusing attention on a single pore, a rather complex situation can be analyzed in a simple manner. Further, the parameters in the model can be approximated from measurement of the pore volume and surface area of the reacted and the unreacted pellet. Comparison with experimental data on the reduction of nickel oxide pellets with carbon monoxide and on the sulfation of calcium oxide provide tests of the model for systems involving structural changes.

CONCLUSIONS AND SIGNIFICANCE

The single-pore model provides a simple means of accounting for changes in pore geometry that occur during reaction. The main parameters of the model are the effective pore length and the effective diffusivity of the product layer. A further important parameter, determined by the characteristics of the chemical system, is the ratio (γ) of the molal volume of the porous product to that of the reactant. For $\gamma = 1$, the pore geometry does not change. For $\gamma < 1$, reaction leads to a more open pore structure. In this case, the single-pore model predicts that the time required to achieve a given conversion is reduced. The system nickel oxide-nickel has a value of

γ of about 0.7, and the experimental results for the reduction of nickel oxide with carbon monoxide agree well with the model predictions. Values of $\gamma > 1$ result in a decrease in average pore radius, and large values of γ can lead to pore-mouth closure which means that the conversion approaches an asymptotic value less than 100%. Such asymptotic conversions have been experimentally observed for hydrofluorination of uranium dioxide and sulfation of calcium oxide. For the latter system, the model predictions agreed reasonably well with the conversion vs. time and conversion vs. porosity data presented by Hartman and Coughlin (1974).

The main advantage of the model is the small number of required parameters. These parameters can be evaluated from a limited amount of conversion-time data, or they may be approximated by measurement of the properties of the reacted and unreacted forms of the pellet.

DESCRIPTION OF THE MODEL

Consider a reaction scheme

$$A(g) + bB(s) \rightarrow pP(g) + gG(s)$$

and suppose that the solid pellet consists of a number of parallel cylindrical pores, each of finite length. Each pore would have some reactant solid (B) associated with it. For prediction of the rate of reaction and conversion-time data, it is sufficient to concentrate attention on a single pore. Thus, the procedure is to analyze reaction in a cylindrical pore of initial radius r and length l and an associated concentric cylindrical solid reactant with an overall radius of λ (see Figure 1*a*). The reaction occurs along the pore walls, resulting in a buildup of product layer. The local radius of the pore itself changes owing to chemical reaction whenever the molal volume of the porous product formed is different from that of the reactant (for example, Figure 1*b*). The model considers diffusion along the axis of the pore, diffusion through the product layer formed upon the pore walls, and surface reaction at the boundary separating the product layer and the solid reactant.

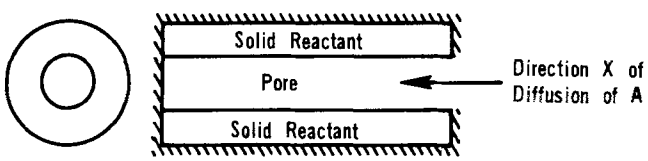

Fig. 1*a*. Schematic representation of the single pore at time $t = 0$.

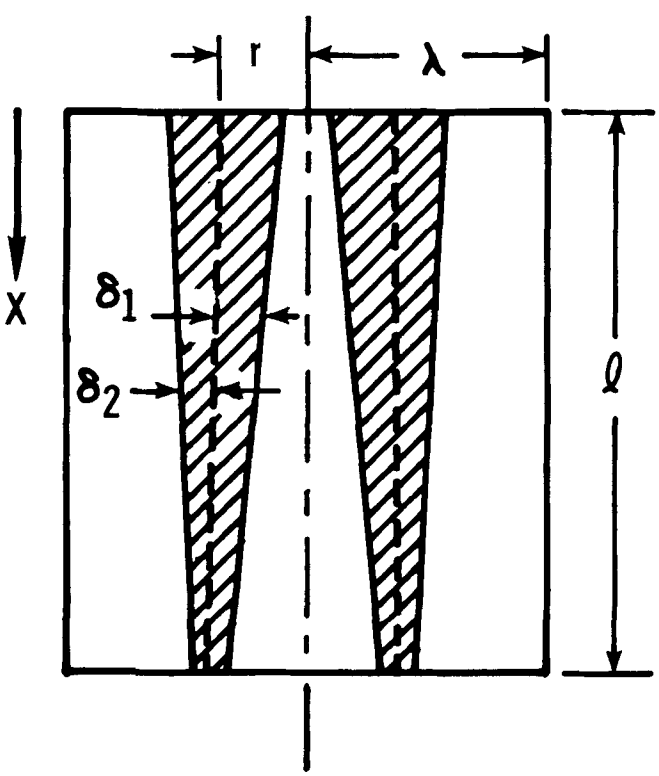

Fig. 1*b*. Geometry of the shrinking-pore case showing the definition of various distance parameters. Dotted line represents position of pore walls at $t = 0$, solid lines at time t. Dashed line represents centerline of original pore.

The main assumptions may be summarized as follows.

1. The pore is cylindrical of finite length l and of uniform original radius r.
2. Each pore has a cylindrical solid associated with it with an overall radius λ.
3. The concentration of gas A does not vary radially in the pore.
4. The concentration of gas A within the solid-product layer is assumed to vary only in the radial direction, and there is no axial diffusion of A in the product layer.
5. The chemical reaction is irreversible and first order with respect to gas A and first order with respect to the interfacial surface of B.
6. Isothermal conditions prevail.
7. External mass transfer resistances are neglected.
8. Solid reactant (A) is nonporous so that the reaction occurs at a sharp interface. This means that the original solid pellet consists only of macropores.

The main differences between this model and model of Szekely and Evans (1970) are that the pore is of finite length so that conversion-time behavior can easily be predicted and that the pore geometry changes with reaction. The main differences with the model of Petersen (1957) are that the products are not entirely gaseous and that diffusion through the product layer (which may be dominating for certain reactions) is accounted for.

MATHEMATICAL FORMULATION

In developing the conversion (of B)-time relation, the first step is to obtain the rate of reaction per unit volume of the pore. Two steps are involved in the reaction process: diffusion through the product layer and

surface reaction. With the pseudo steady state hypothesis, the overall rate is equal to the rate of the individual steps. Hence, the rate of reaction of A for a differential volume of pore of length Δx is

R_A (g mole/sec)

$$= 2\pi(\Delta x)C \left[\frac{1}{k(r+\delta_2)} + \frac{\ln \frac{r+\delta_2}{r-\delta_1}}{D_e} \right]^{-1} \quad (1)$$

The quantities δ_1 and δ_2 refer to the thickness of the product layer on either side of the initial position of the pore wall (see Figure 1*b* for definitions).

The concentration profile of gas A in the pores as a function of axial distance along the pores $C = f(x)$ can be established by a mass balance using Equation (1) for the rate of chemical reaction:

$$D\frac{d}{dx}\left[(r-\delta_1)^2 \frac{dC}{dx} \right] = 2C \left[\frac{1}{k(r+\delta_2)} + \frac{\ln \frac{r+\delta_2}{r-\delta_1}}{D_e} \right]^{-1} \quad (2)$$

or

$$D(r-\delta_1)^2 \frac{d^2C}{dx^2} - 2(r-\delta_1)D\frac{d\delta_1}{dx}\frac{dC}{dx} = 2C \left[\frac{1}{k(r+\delta_2)} + \frac{\ln \frac{r+\delta_2}{r-\delta_1}}{D_e} \right]^{-1} \quad (3)$$

The first term on the left side is the normal term arising from diffusion in the x direction, while the second term occurs because of the changes in the pore area in the x direction. In general, $d\delta_1/dx$ is small so that the second term can usually be neglected. In Equations (2) and (3), δ_1 and δ_2 are, for the general case, functions of x as well as of time. In Equation (3), D is the diffusivity of gas A within the pore and includes contributions of both bulk diffusion and Knudsen diffusion.

The variation of δ_1 and δ_2 with time can be formulated in the following way. The total thickness of the product layer is $\delta = \delta_1 + \delta_2$. If this thickness changes by $\Delta\delta$ in time Δt, the volume of the product formed in time Δt is $2\pi(r+\delta_2)(\Delta\delta)(\Delta x)$. If ρ_G is the solid (skeletal) density of the product and ϵ_G the porosity, the rate of product formation is

$$2\pi\frac{\rho_G}{M_G}(1-\epsilon_G)(r+\delta_2)\Delta x\frac{\Delta\delta}{\Delta t} \text{ in g mole/s}$$

and this would be equal to $g(R_A)$ by stoichiometry. Hence, we obtain

$$\frac{d\delta}{dt} = \frac{d\delta_1}{dt} + \frac{d\delta_2}{dt} = \frac{gM_G}{\rho_G(1-\epsilon_G)}\frac{C}{(r+\delta_2)} \left[\frac{1}{k(r+\delta_2)} + \frac{\ln \frac{r+\delta_2}{r-\delta_1}}{D_e} \right]^{-1} \quad (4)$$

An additional equation relating δ_1 and δ_2 is needed to complete the formulation of the model. This can be obtained from the requirement of conservation of mass during reaction. The product has a thickness $\delta_1 + \delta_2$ at a given time, and this product has been formed from

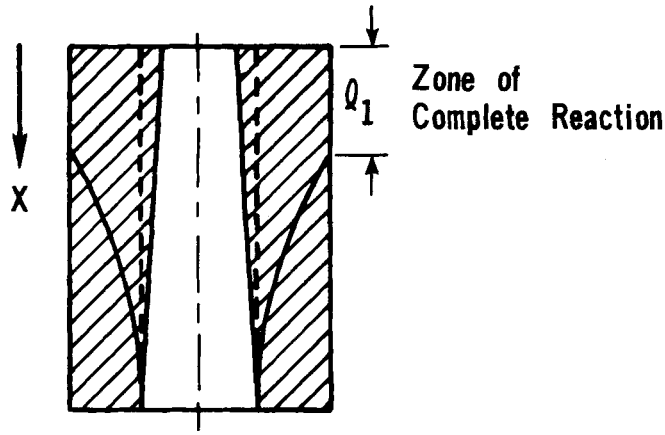

Fig. 1c. Single pore with region of complete reaction.

a reactant solid of thickness δ_2. Since mass must be conserved

$$\text{moles of } B = \frac{b}{g} \text{ (moles of } G)$$

or

$$\frac{\rho_B}{M_B}[(r+\delta_2)^2 - r^2] = \frac{b}{g}\frac{\rho_G}{M_G(1-\epsilon_G)}[(r+\delta_2)^2 - (r-\delta_1)^2]$$

Simplifying, we get

$$(r-\delta_1)^2 = (1-\gamma)(r+\delta_2)^2 + \gamma r^2 \quad (5)$$

where γ is defined as

$$\gamma = \frac{\rho_B}{M_B}\frac{g}{b}\frac{M_G}{\rho_G(1-\epsilon_G)} \quad (6)$$

For $\gamma = 1$, Equation (5) shows that δ_1 is zero, which means that there is no change in pore geometry with time. Equation (5) can also be expressed in differential form to achieve some computational advantages:

$$(r-\delta_1)\frac{d\delta_1}{dt} = (\gamma-1)(r+\delta_2)\frac{d\delta_2}{dt} \quad (5a)$$

Equation (5*a*) indicates that for $\gamma > 1$, δ_1 increases with time, which corresponds to a decrease in the pore radius with time. For $\gamma < 1$, δ_1 will be negative, and physically this corresponds to an increase in pore radius.

The boundary and initial conditions are

$$\text{At } x = 0 \quad C = C_o \quad (7)$$

$$\text{At } x = l \quad \frac{dC}{dx} = 0 \quad (7a)$$

$$\text{At } t = 0 \quad \delta_1 = 0 = \delta_2 \quad (8)$$

The local conversion η of the solid (B) depends on δ_2 and is given by

$$\eta(x) = 1 - \frac{\lambda^2 - (r+\delta_2)^2}{\lambda^2 - r^2} \quad (9)$$

The average conversion for the entire pore is

$$\bar{\eta} = \frac{1}{l}\int_o^l \left[1 - \frac{\lambda^2 - (r+\delta_2)^2}{\lambda^2 - r^2} \right] dx \quad (10)$$

Under certain conditions, a zone of completely reacted solid will develop near $x = 0$ (Figure 1*c*). This occurs

when the value of δ_2 becomes equal to $\lambda - r$. For this case, Equation (3) has to be solved separately for the two zones 0 to l_1 and l_1 to l. For 0 to l_1, the rate term on the right-hand side of Equation (3) would be equal to zero, since no solid reactant is available for reaction in this zone.

DIMENSIONLESS VARIABLES AND PARAMETERS

Equations (3), (4), and (5*a*) were cast in dimensionless form using the following variables:

$$C^* = \frac{C}{C_o}, \quad x^* = \frac{x}{l}, \quad \delta_1{}^* = \frac{\delta_1}{r}, \quad \delta_2{}^* = \frac{\delta_2}{r}$$

$$\tau = \left(\frac{tD}{r^2}\right) \frac{gM_G C_o}{\rho_G(1 - \epsilon_G)}$$

The resulting dimensionless equations are

$$\frac{d^2C^*}{dx^{*2}} - \frac{2}{(1 - \delta_1{}^*)}\left(\frac{d\delta_1{}^*}{dx^*}\right)\left(\frac{dC^*}{dx^*}\right) = 2\frac{l^2}{r^2}\frac{C^*}{(1 - \delta_1{}^*)^2}$$

$$\left[\frac{1}{Bi(1 + \delta_2{}^*)} + \frac{\ln\left(\frac{1 + \delta_2{}^*}{1 - \delta_1{}^*}\right)}{(D_e/D)}\right]^{-1} \tag{11}$$

$$\frac{d\delta_1{}^*}{d\tau} + \frac{d\delta_2{}^*}{d\tau} = \frac{C^*}{(1 + \delta_2{}^*)}$$

$$\left[\frac{1}{Bi(1 + \delta_2{}^*)} + \frac{\ln\left(\frac{1 + \delta_2{}^*}{1 - \delta_1{}^*}\right)}{(D_e/D)}\right]^{-1} \tag{12}$$

and

$$(1 - \delta_1{}^*)\frac{d\delta_1{}^*}{d\tau} = (\gamma - 1)(1 + \delta_2{}^*)\frac{d\delta_2{}^*}{d\tau} \tag{13}$$

where

$$Bi = \frac{kr}{D}$$

In dimensionless form, Equation (10) for the average conversion becomes

$$\bar{\eta} = \int_o^1 \left[1 - \frac{1 - \left(\frac{r}{\lambda}\right)^2 (1 + \delta_2{}^*)^2}{1 - \left(\frac{r}{\lambda}\right)^2}\right] dx^* \tag{14}$$

The main parameters are pore radius r, length of the pore l, the outer radius of the concentric associated solid λ, the effective diffusivity in the solid product layer D_e, and the rate constant for surface reaction k. Approximate values of these parameters can be estimated by the methods listed in the following paragraphs. Such estimates are useful for predicting conversion-time results in the absence of experimental reaction data and as a starting point for more accurate estimates by comparison with the experimental data.

Average Pore Radius r

Since the pore is assumed to be cylindrical, the average pore radius for a monodisperse pellet may be estimated from the expression

$$r = 2\frac{V_g}{S_g} \tag{15}$$

Since V_g is related to the initial porosity ϵ_o, the average pore radius can also be expressed as

$$r = \frac{2\epsilon_o}{\rho_p S_g} \tag{16}$$

where ρ_p is the density of the pellet.

Radius of the Associated Solid λ

The porosity of the single pore at $t = 0$ is

$$\epsilon_o = \frac{\pi r^2}{\pi \lambda^2} \tag{17}$$

Assuming that the porosity of the single pore at $t = 0$ is the same as that of the unreacted solid, we have

$$\frac{\lambda}{r} = \frac{1}{\sqrt{\epsilon_o}} \tag{18}$$

Effective Pore Length l

This parameter is important since it determines the significance of diffusional gradients within the single pore. It is rational to choose it in such a way that the original pellet and the single pore of the model have the same diffusional characteristics. Such characteristics of the original pellet depend on the Thiele modulus. At zero time, this is defined for a spherical geometry as

$$\frac{R}{3}\left(\frac{k\rho_p S_g \tau_f}{D\epsilon_o}\right)^{1/2}$$

Equation (11) for a single pore at $\tau = 0$, (if we neglect the term involving $d\delta_1{}^*/dx^*$) gives

$$\frac{d^2C^*}{dx^{*2}} = 2\frac{l^2}{r}\left(\frac{k}{D}\right)C^* \tag{19}$$

With average pore radius from Equation (16), Equation (19) becomes

$$\frac{d^2C^*}{dx^{*2}} = \frac{l^2 k\rho_p S_g}{\epsilon_o D} C^* \tag{20}$$

Thus, the equivalent Thiele modulus of the single pore is $l(k\rho_p S_g/\epsilon_o D)^{1/2}$. In order to have the same internal diffusional resistance, the effective length of the single pore of the model must be defined as

$$l = \frac{R}{3}\sqrt{\tau_f} \tag{21}$$

The definition of l by Equation (21) ensures that the rate predicted by the single-pore model and that for a spherical pellet, at time $t = 0$, are the same for the same value of the rate constant k.

The tortuosity factor may be predicted, as a first approximation, by the random pore model (Wakao and Smith, 1962). Thus, if the pore structure of the original pellet is monodispersed, the effective pore length is given by

$$l = \frac{R}{3\sqrt{\epsilon_o}} \tag{22}$$

Effective Diffusivity Through the Product Layer D_e

This key parameter is best obtained from experimental conversion-time data. In the absence of such data, an approximate value can be predicted using the random pore concept. By this method, D_e is related to the porosity of the product layer ϵ_G by the following equation:

$$D_e = D\epsilon_G{}^2 \tag{23}$$

Note that D_e is not necessarily equal to $D_e\epsilon_G/\tau_G$ since D

may not be the same in the main pores as in the porous, product layer. The value of ϵ_G can be obtained from the porosity of the completely reacted solid ϵ_f. The completely reacted solid consists of the macropores arising from the original pores and the micropores in the product layer. The total porosity of the completely reacted solid depends on the local pore radius of the reacted solid and is given by

$$\epsilon_f = \int_0^1 \{\epsilon_0(1-\delta_1^*)^2 + \epsilon_G[1-\epsilon_0(1-\delta_1^*)^2]\}dx^* \tag{24}$$

An approximate value of ϵ_G in terms of ϵ_f, obtained by neglecting structural changes, is given by

$$\epsilon_G \simeq \frac{\epsilon_f - \epsilon_0}{1-\epsilon_0} \tag{25}$$

Equation (25) is valid exactly for $\gamma = 1$ and may serve as a starting guess for other cases.

Reaction Rate Constant k

This is the one parameter that must be obtained from experimental reaction data. It may be determined by considering the rate of reaction at $t = 0$. At this point, the conversion is zero so that the thickness of the product layer is negligible. Equation (20) is now applicable, and the rate of reaction is given by [Equation (1)]

$$(R_A)_{t\to 0} = C_o k(2\pi r l)(EF) \tag{26}$$

where EF is the effectiveness factor for the single pore at $t = 0$. It is given by

$$EF = \frac{\tanh\phi}{\phi} \tag{27}$$

and

$$\phi = l\left(\frac{k\rho_p S_g}{\epsilon_o D}\right)^{1/2} \tag{28}$$

Provided that EF can be determined, Equation (26) provides an expression for the rate in terms of k. For the case of no diffusional resistance within the pore ($\phi < 0.2$), the value of EF is about unity. For the other extreme of large diffusional resistances ($\phi > 3$), $EF = 1/\phi$, and Equation (26) takes the form

$$(R_A)_{t\to 0} = \pi r C_o \sqrt{2kDr} \tag{29}$$

Only for intermediate values of ϕ need Equation (27) be used.

Comparison of the experimentally observed initial rate with Equation (26) provides an estimate for the reaction rate constant.

MAXIMUM CONVERSION OF SOLID

In many gas-solid reactions, the maximum conversion of the solid reactant approaches a constant value less than 100%. This can be explained on the basis of the structural changes of the pores, and the maximum conversion can be predicted for a solid reactant of given porosity. The maximum conversion is reached when pore closure occurs. Consider, for simplicity, a pore with no diffusional resistance ($\phi < 0.2$). When pore closure occurs, $\delta_1^* = 1$, and Equation (5) gives

$$(1+\delta_2^*)^2_{\max} = \frac{\gamma}{\gamma - 1} \tag{30}$$

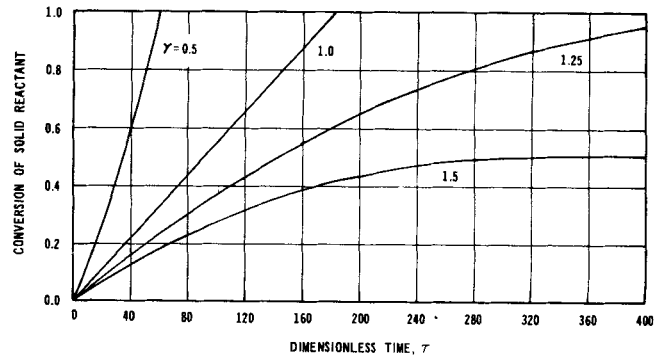

Fig. 2. Conversion vs. time for various values of γ for $Bi = 0.01$, $\epsilon_0 = 0.18$, and $D_e/D = 0.0625$ and for no diffusional resistance in the pore ($\phi < 0.2$).

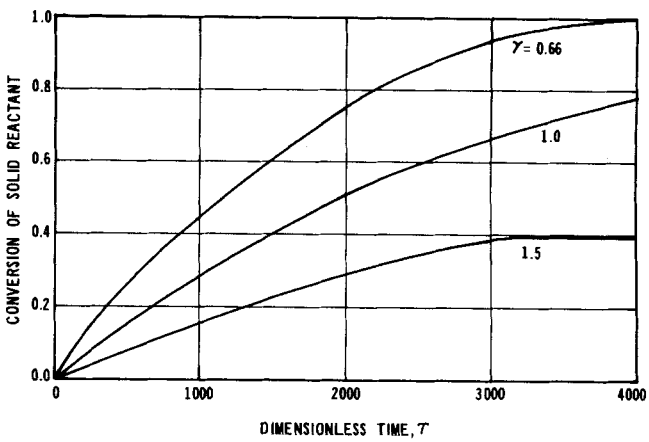

Fig. 3. Influence of γ on conversion for the case when pore diffusion is important for $Bi = 2 \times 10^{-6}$, $D_e/D = 10^{-4}$, $\epsilon_0 = 0.64$, l/r 1 200.

Using this result in Equation (9) or (10), and using Equation (18), we get for the maximum conversion

$$(\bar{\eta})_{\max} = 1 - \frac{1-\epsilon_o\dfrac{\gamma}{\gamma-1}}{1-\epsilon_o} \tag{31}$$

Equation (31) is applicable only for $\gamma > 1$.

There is a further restriction that conversion can not be greater than 100%. This occurs at $\epsilon_o = (\gamma - 1)/\gamma$. Thus, complete conversion of the solid is ensured, provided the initial porosity of the pellet is greater than $(\gamma - 1)/\gamma$ and for the case of no diffusional resistance in the pore. When concentration gradients exist in the pores, the porosity has to be still higher in order to achieve complete conversion. An interesting application of this to the sulfation reaction of calcium carbonate follows from the work of Hartman and Coughlin (1974) and is discussed later.

RESULTS

Equations (11) to (14) with Equations (7), (7a), and (8) can be solved numerically for the conversion as a function of time and the several parameters. Such calculations were made to show the effects of key properties of the reaction system.

Influence of γ on Conversion and on Pore Structure

The influence of γ was studied over the range 0.5 to 1.5 for cases without and with pore diffusional resistances. The results are shown in Figure 2 and 3 as plots of conversion vs. time. It is seen that the time required to achieve a given conversion is reduced as γ

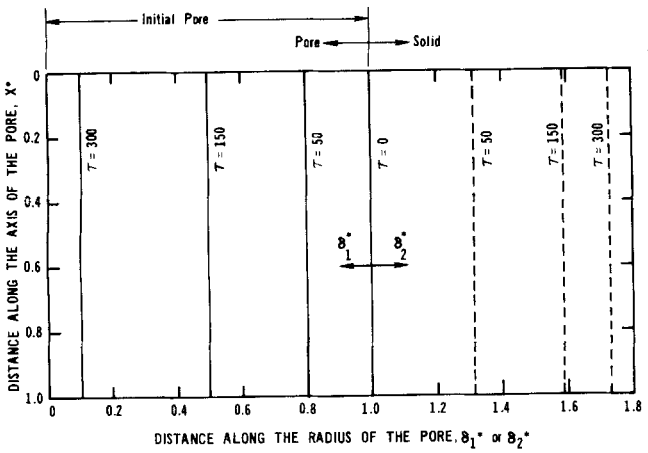

Fig. 4. Development of pore closure for no diffusional resistance, $Bi = 0.01$, $\gamma = 1.5$, $\epsilon_0 = 0.18$, $D_e/D = 0.0625$, $l/r = 1\,200$. Solid lines indicate pore wall, and dotted lines indicate reaction interface.

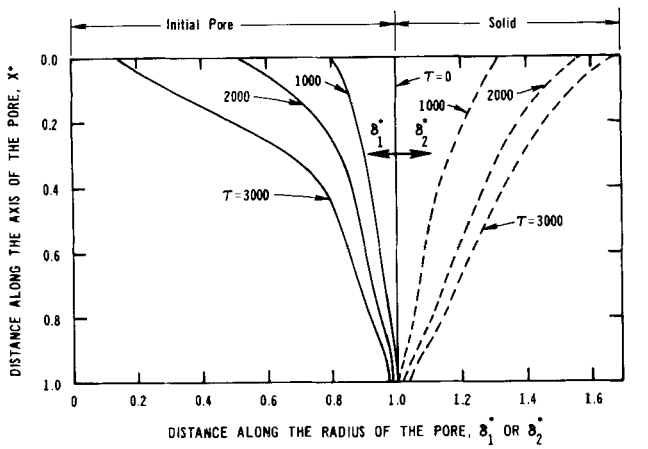

Fig. 5. Development of pore closure for case of significant diffusional resistance, $Bi = 2 \times 10^{-6}$, $\gamma = 1.5$, $D_e/D = 10^{-4}$, $l/r = 1\,200$, $\epsilon_0 = 0.35$. Solid lines indicate pore wall, and dotted lines indicate reaction interface.

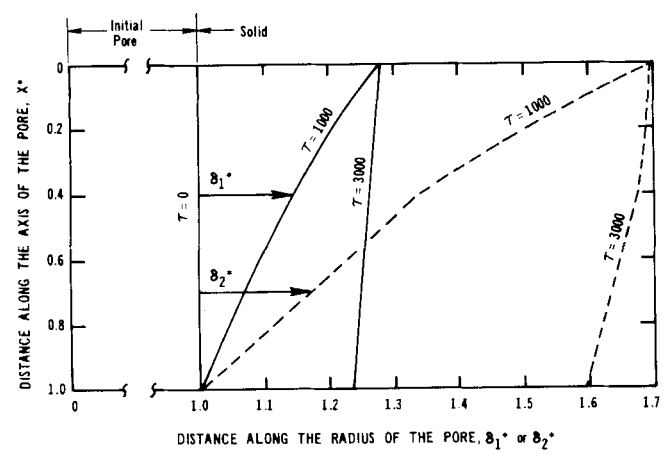

Fig. 6. Development of an open pore structure for $\gamma = 0.66$. Solid lines indicate pore wall, and dotted lines indicate reaction interface, $Bi = 2 \times 10^{-6}$, $D_e/D = 10^{-4}$, $\epsilon_0 = 0.35$, $l/r = 1\,200$.

is reduced. For $\gamma = 1.5$, and no diffusional resistances, the conversion reaches a maximum of 51% in agreement with Equation (31). The decrease in pore radius with time for this case is shown in Figure 4. As there are no diffusional effects, the rate of reaction is uniform along the pore walls and results in a uniform product layer thickness. Contrast this with the situation in Figure 5 which is applicable to a case with significant diffusional resistance. The rate of reaction is now very large

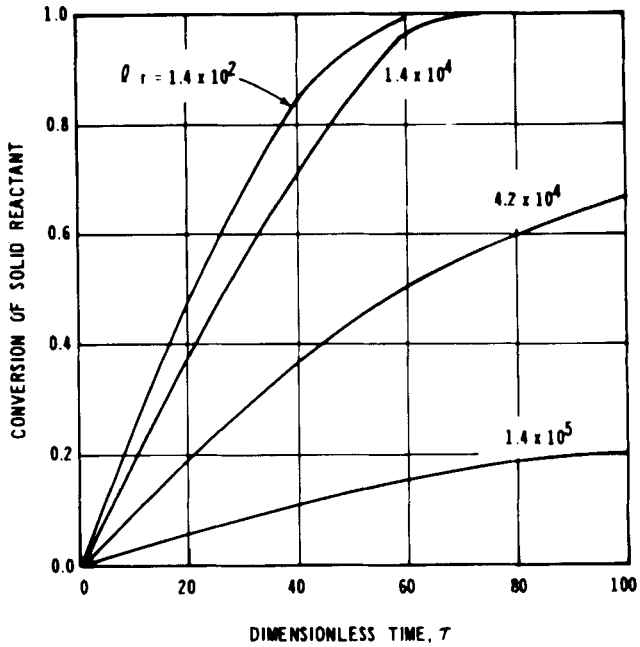

Fig. 7. Effect of pore length on the conversion-time relationship for $Bi = 1.6 \times 10^{-9}$, $\epsilon_0 = 0.6$, $\gamma = 1.9$, and $D_e/D = 10^{-4}$.

near the pore mouth, while it is low at the end of the pore. As a result, the product growth is mainly near the mouth of the pore, and when pore closure occurs, a significant amount of material can remain unreacted near the end of the pore. For the parameter values used in Figure 4, this gives an asymptotic conversion of 39%.

For $\gamma < 1$, a more open pore structure develops with time. Such behavior is shown in Figure 6 for $\gamma = 0.66$. The average pore radius increases with time. This increase is larger near the mouth than the end whenever there are diffusional gradients within the pore. The increase facilitates diffusion, resulting in a reduction in time for complete conversion.

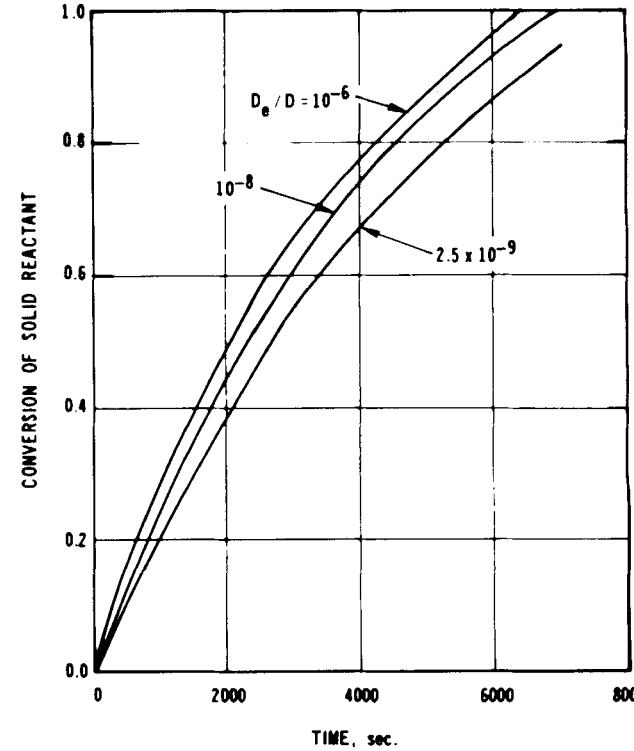

Fig. 8. Influence of diffusion through product layer (D_e/D) on the conversion-time relationship for the reaction-dominated case; $Bi = 2 \times 10^{-8}$, $\gamma = 0.66$, $\epsilon_0 = 0.35$, $l/r = 1.88 = 10^4$.

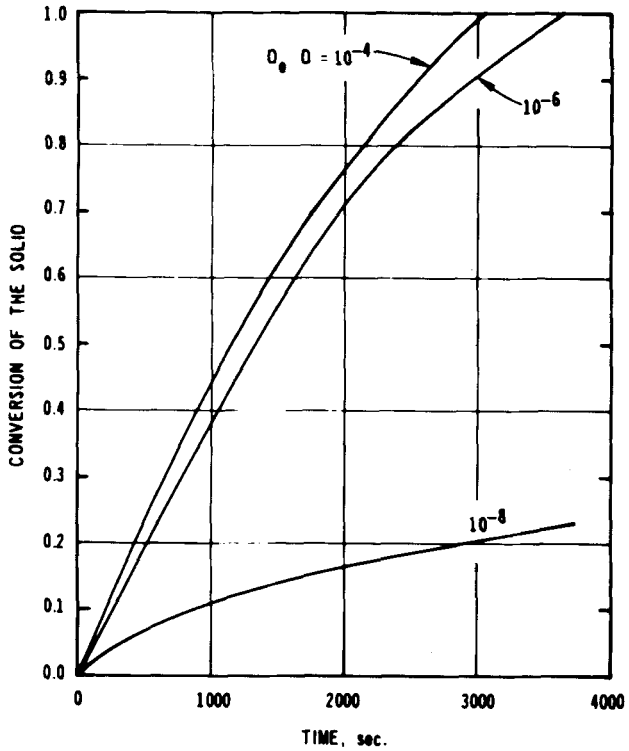

Fig. 9. Influence of D_e/D when product layer diffusion controls the rate; $Bi = 2 \times 10^{-6}$, $\gamma = 0.66$, $\epsilon_0 = 0.35$, $l/r = 1\,200$.

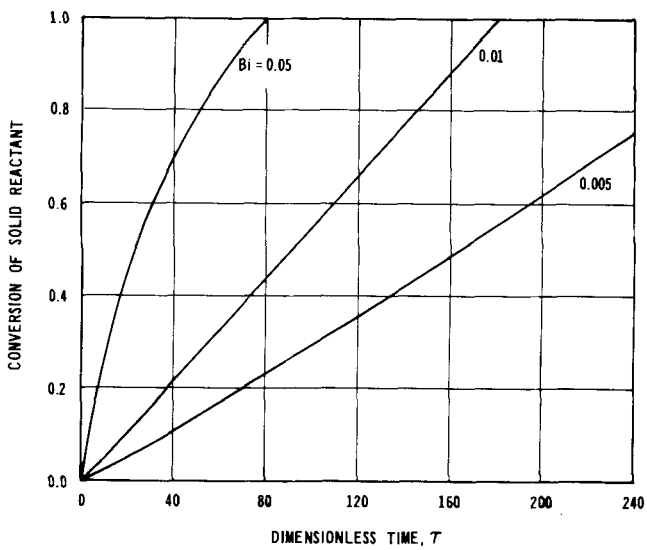

Fig. 10. Influence of intrinsic reaction rate (Bi) on the conversion-time relationship for the case when pore diffusion is unimportant; $D_e/D = 0.66$, $\gamma = 1.0$, $\epsilon_0 = 0.18$.

Influence of Effective Pore Length

The influence of pore length was studied by varying the ratio l/r over the range 1 400 to 140 000. For small values of l/r (1.4×10^3 in Figure 7), diffusional effects are not important. Hence, a tenfold change in this parameter causes only a nominal change in conversion (Figure 7). The diffusional gradients in the pore become dominant for l/r greater than 1.4×10^4 for the chosen values of the other parameters. A further tenfold increase in l/r causes the conversion to drop drastically (Figure 7). Thus the parametric sensitivity of the model to effective pore length is largest when ϕ is large.

Influence of Diffusion Through the Product Layer

The importance of the effective diffusivity through the product layer depends on the relative resistances of diffusion through the product layer and surface reaction.

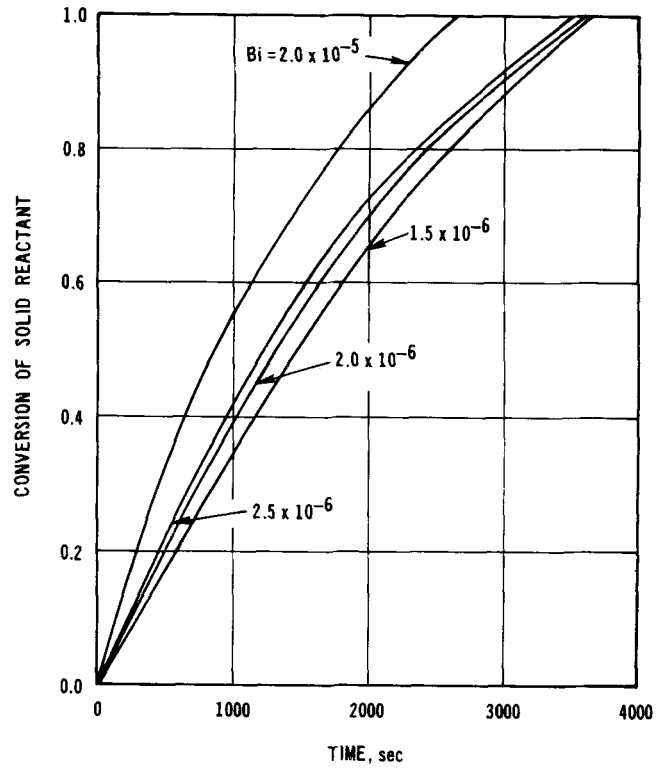

Fig. 11. Influence of intrinsic reaction rate when pore diffusion controls the rate; $D_e/D = 10^{-6}$, $\gamma = 0.66$, $\epsilon_0 = 0.35$, $l/r = 1\,200$.

At the start of the reaction, the process is entirely governed by surface reaction. As the product layer thickness increases, the diffusional effect is important whenever D_e/D is small in comparison with the magnitude of Bi. For fast surface reactions and low porosity of the product layer, diffusion through the product layer is dominating and D_e becomes an important parameter. The sensitivity of the model to variations in D_e was studied for two cases: relatively slow reaction with $Bi = 2 \times 10^{-8}$ (Figure 8) and relatively fast reaction ($Bi = 2 \times 10^{-6}$, Figure 9). Figure 8 shows that changes in D_e do not affect the conversion-time relationship significantly; a hundredfold variation in D_e affects the conversion but slightly. In contrast, the system in the second case is very sensitive to changes in D_e/D below $D_e/D \approx 10^{-6}$ (Figure 9). However, for $D_e/D > 10^{-6}$, the contribution of diffusional resistances is greatly reduced and so is the sensitivity of the model to variations in D_e.

Influence of Reaction Rate Constant

The effect of k was studied by varying Bi for two values of D_e/D, 0.66 (Figure 10) and 10^{-6} (Figure 11). When $D_e/D = 0.66$, the product layer would be highly porous so that the surface reaction controls the process. The influence of Bi on the conversion under such circumstances is very significant. A value of $D_e/D = 10^{-6}$ would be representative of systems where a relatively impervious product layer was formed. Hence, reaction resistances would be small, and changes in Bi do not greatly affect the conversion, as shown in Figure 11.

The Biot numbers in Figures 10 and 11 range from 0.05 to 2×10^{-6}. Practical values of Bi probably vary widely; for example, in the nickel oxide system (Figure 12) $Bi = 2 \times 10^{-8}$, and for the calcium oxide-sulfur dioxide reaction (Figure 13) $Bi = 1.38 \times 10^{-5}$. The large values in Figure 10 would correspond to a very slow intrinsic reaction rate. More likely values are those in the 10^{-5} to 10^{-8} region.

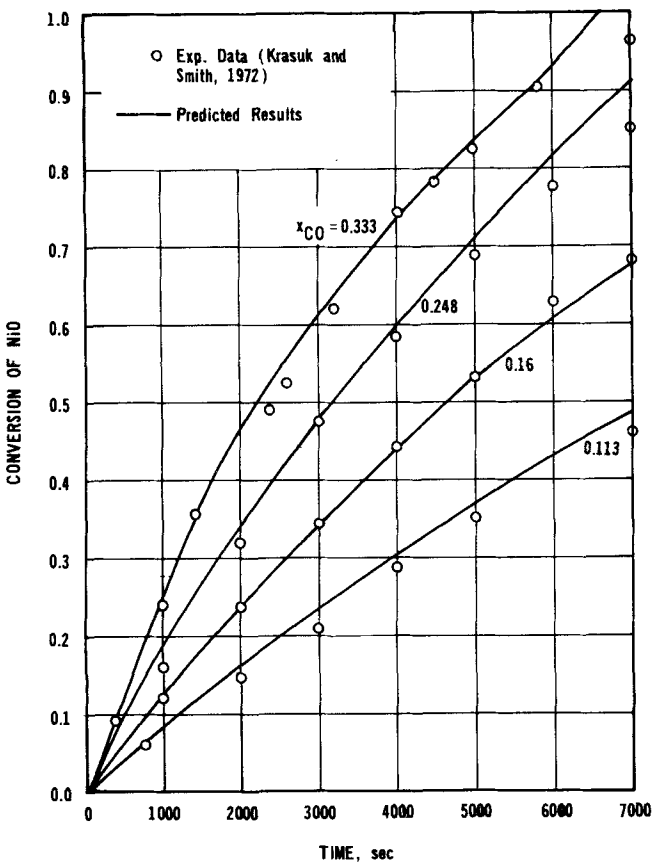

Fig. 12. Application to the reduction of nickel oxide with carbon monoxide.

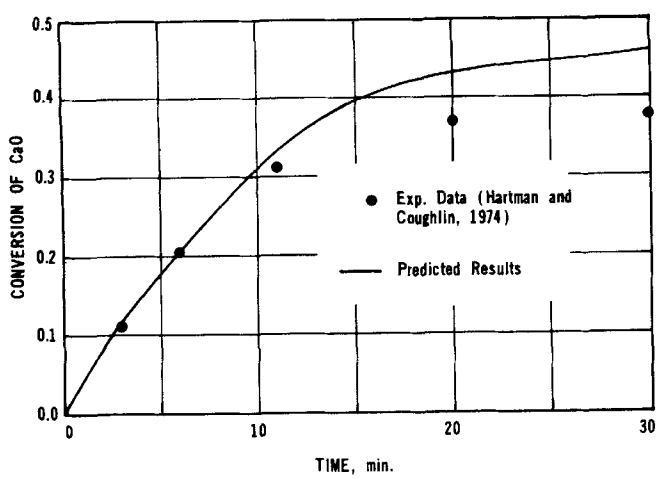

Fig. 13. Application to the sulfation of calcium oxide.

APPLICATIONS

Reduction of Nickel Oxide with Carbon Monoxide

Few publications on gas-solid reactions include sufficient information about physical properties of the solid reactant to apply reaction models. Krasuk and Smith (1972) in their study of nickel oxide reduction with carbon monoxide, in a single pellet, stirred reactor, measured such properties of nickel oxide and the reaction product as porosity, pore volume, and surface area. The data relevant to application of the single-pore model are as follows

1. Reaction rate constant (estimated by Krasuk and Smith from the initial rate data) = 5.5×10^{-4} cm/s.
2. Diffusivity within the pore $D = 0.715$ cm^2/s.
3. Initial porosity of the reactant $\epsilon_o = 0.35$.
4. Average pore diameter = 0.521×10^{-4} cm.
5. Temperature = 767°C.
6. Mole fraction of carbon monoxide = 0.113 to 0.333.
7. Radius of the pellet = 0.85 cm.
8. Effective pore length (estimated from $R/3\sqrt{\epsilon_o}$) = 0.499 cm.
9. $\gamma = 0.658/(1 - \epsilon_G) \simeq 0.658$ since the porosity measurement on the final product indicated that the porosity of the product layer is likely to be very small.

The predictions of the theory using these values of the parameters were compared with the experimental data. The value of D_e which gave the best agreement with the data was 0.715×10^{-8} cm^2/s. The predicted and experimental conversions are shown in Figure 12 for various mole fractions of carbon monoxide in the gas around the pellet. It is seen that the single-pore model predicts the data reasonably well. The low value of D_e in the product layer indicates that the product is almost impermeable to the reactant. If we used the random pore model, this diffusivity would correspond to a porosity of about 0.01% in the product layer. Such a low value is in agreement with the experimental observation that the porosity at the end of the run did not increase greatly, although the pore size was increasing. The final average pore diameter determined from the measured values of V_g and S_g was 0.860×10^{-4} cm. The predicted result (average value for the entire length of pore) was 0.690×10^{-4} cm.

Sulfation of Calcium Carbonate

Hartman and Couglin (1974) studied the reaction of sulfur dioxide with calcium carbonate, which occurs in two successive steps:

$$CaCO_3 \rightarrow CaO + CO_2$$

$$CaO + SO_2 + \tfrac{1}{2}O_2 \rightarrow CaSO_4$$

The first reaction is assumed to be instantaneous, while the second reaction takes place at a finite rate. The molal volumes of the various species are as follows:

$$CaCO_3 = 36.9, \quad CaO = 16.9, \quad CaSO_4 = 52.2, \quad \text{cm}^3/\text{mole}$$

Thus, the first reaction leads to an open pore structure. If the starting material, calcium carbonate, is essentially nonporous and decomposes instantly to give calcium oxide, the porosity of calcium oxide formed is 1 − 16.9/36.9, or 0.542. The second reaction has a value of γ of about 3.08. The maximum theoretical conversions of calcium oxide for this γ, as calculated from Equation (31), is 57%. The porosity of the product formed as a result of the second reaction was measured by Hartman and Coughlin (1974) and found to approach zero for conversions approaching 57%. The authors also reported fractional conversion of calcium oxide with time. This conversion reached an asymptotic value of about 37%, far less than the theoretical maximum. One possible explanation is diffusional resistance within the pores. We have compared the experimental data with those predicted by the single-pore model using the following values for the parameters.

1. Reaction rate constant = 0.102 cm/s (estimated from the initial rate data).
2. Average pore radius = 1.02×10^{-4} cm (reported by Hartman and Couglin, 1974).
3. Diffusivity in the pore $D = 0.75$ cm^2/s. (molecular diffusivity of sulfur dioxide in flue gas).
4. Porosity of the initial solid, $\epsilon_o = 0.535$.

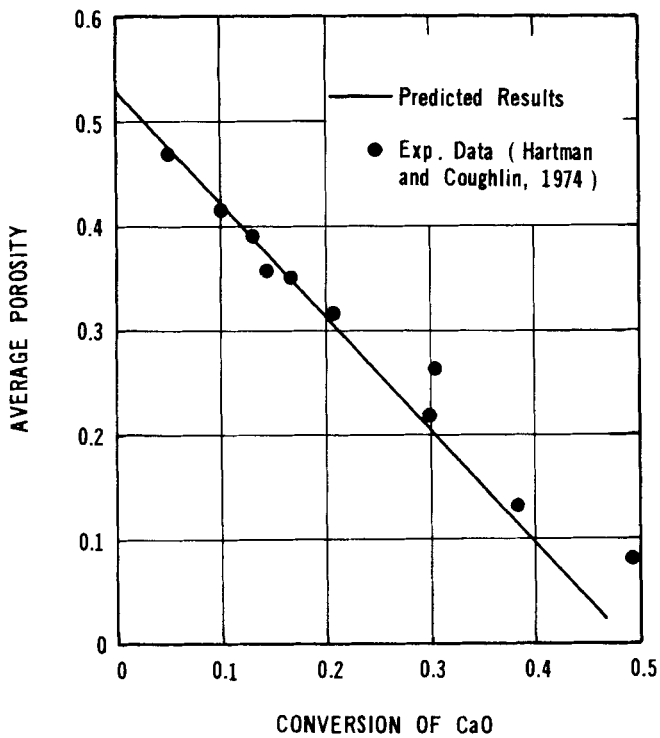

Fig. 14. Decrease in average porosity of calcium oxide pellet with conversion.

5. Average radius of the pellet = 0.565 cm.

6. Porosity of the product layer ϵ_G (from D_e and random pore model) = 0.001.

7. Diffusivity in product layer D_e (chosen to give best agreement with data) = 0.75×10^{-6} cm²/s.

8. $\gamma = 3.08$.

9. Temperature = 850°C.

10. Effective pore length (from $R/3\sqrt{\epsilon_o}$) = 0.257 cm.

The model predictions agreed well with the experimental data in the early stages of reaction, as shown in Figure 13. Since the model takes into account diffusion within the pores, the asymptotic ($t \rightarrow \infty$) conversion is 46%, much less than the theoretical maximum. The experimental value is somewhat lower, 37%. This could be the result of other structural changes such as sintering. Predicted values of the average porosity of the pellet for various conversions of calcium oxide were also made using Equation (24). The comparison of predicted and experimental results (Figure 14) is good.

These examples show that the single-pore model may have some utility for accounting for the effect of structural changes in the porous solid as a result of reaction. Particularly, the model seems valuable for predicting maximum conversions less than 100%.

NOTATION

b = stoichiometric coefficient of solid reactant
Bi = Biot number for reaction at the pore walls, defined as $k\,r/D$
C^* = dimensionless concentration of gas A, C/C_o
C = concentration of gas A at any point within the pore, g mole/cm³
C_o = concentration of gas A in the external fluid surrounding the pellet, g mole/cm³
D = diffusivity of gas in the pores, cm²/s
D_e = effective diffusivity of gas within the product layer, cm²/s
g = stoichiometric coefficient of solid product
l = effective pore length, cm
k = surface reaction rate constant, cm/s
M_B = molecular weight of species B
M_G = molecular weight of species G
p = stoichiometric coefficient of gaseous product
r = radius of the pore at $t = 0$, cm
R = radius of the pellet, cm
R_A = rate of disappearance of gaseous reactant A, g mole/s
S_g = surface area of the pellet per unit mass, cm²/g
t = time, s
V_g = pore volume of the pellet per unit mass, cm³/g
x = axial distance in the pore, measured from pore mouth, cm
x^* = dimensionless distance, defined as x/l

Greek Letters

γ = parameter defined as $\dfrac{g\,\rho_B\,M_G}{b\,\rho_G\,M_B(1-\epsilon_G)}$
δ = total thickness of the product layer ($\delta_1 + \delta_2$)
δ_1 = thickness of that part of the product layer measured from the initial position of the pore walls to the pore wall at any time, cm
δ_2 = thickness of that part of the product layer between the initial position of the pore wall and the reaction interface, cm
δ_1^* = dimensionless thickness, δ_1/r
δ_2^* = dimensionless thickness, δ_2/r
ϵ_o = porosity of the pellet at $t = 0$
ϵ_f = total porosity of the completely reacted solid
ϵ_G = porosity of the product layer (layer of product G)
ρ_p = density of the pellet, g/cm³
ρ_B = density of the solid B, g/cm³
ρ_G = density of the solid G, g/cm³
η = local conversion
$\bar{\eta}$ = average conversion
λ = radius of the solid reactant associated with a pore, cm
τ = dimensionless time, defined as $\left(\dfrac{t\,D}{r^2}\right)\dfrac{g\,M_G\,C_o}{\rho_G(1-\epsilon_G)}$
τ_f = tortuosity factor of the original pellet
ϕ = Thiele modulus for the pore defined by Equation (28)

LITERATURE CITED

Calvelo, A., and J. M. Smith, "Intrapellet Transport in Gas-Solid Non-Catalytic Reactions," *Proceedings of Chemeca 70*, Paper 3.1, Butterworths, Australia (Aug., 1971).

Chu, C., "Parallel Plate Model for Non-Catalytic Gas-Solid Reactions," *Chem. Eng. Sci.*, **27**, 367 (1972).

Hartman, M., and R. W. Couglin, "Reaction of Sulfur Dioxide with Limestone and the Influence of Pore Structure," *Ind. Eng. Chem. Process Design Develop.*, **13**, 248 (1974).

Hashimoto, K., and P. L. Silveston, "Gasification, Part I, Isothermal Kinetic Control Model for a Solid with a Pore-Size Distribution," *AIChE J.*, **19**, 259 (1973).

———, "Part II. Extension to Diffusion Control," *ibid.*, 268 (1973*a*).

Krasuk, J. H., and J. M. Smith, "Kinetics of Reduction of Nickel Oxide with Carbon Monoxide," *ibid.*, **18**, 506 (1972).

Petersen, E. E., "Reaction of Porous Solids," *ibid.*, **3**, 443 (1957).

Szekely, J., and J. W. Evans, "A Structural Model for Gas-Solid Reactions with a Moving Boundary," *Chem. Eng. Sci.*, **25**, 1091 (1970).

Wakao, N., and J. M. Smith, "Diffusion in Catalyst Pellets," *ibid.*, **17**, 825 (1962).

Manuscript received November 9, 1976; revision received February 15, and accepted February 22, 1976.